

Chapter II

THE ROCHE MODEL

One of the fundamental problems of the astronomy of close binary systems is to investigate the equilibrium forms of their components, of arbitrary structure, distorted by rotation and tides, defined as the surfaces over which the potential of all forces acting within the system remain constant. Should we insist that such results be applicable to stars of any structure, the problem of the equilibrium forms has so far been solved only to a limited degree of accuracy—insufficient for an interpretation of the observed phenomena of very close systems. The aim of the present chapter will, however, be to demonstrate that if this latter requirement is given up, and the density concentration of the stars constituting our binary is allowed to approach infinity, their shape can be described in a closed *algebraic* form, which is *exact* for any such configuration *irrespective of the proximity of its components or their mass ratio*. Such a model is generally known in the literature, under the name of its originator, as the *Roche Model*; and the aim of the present chapter will be to summarize its most important geometrical and other properties which should be of interest for the students of close binary systems.

II.1 Roche Model: A Definition

In order to introduce to the reader such a model, let $m_{1,2}$ denote the masses of the two components of a close binary system; and R , the separation of their centres of mass. Suppose, moreover, that the positions of these centres are referred to a rectangular system of Cartesian coordinates, with the origin at the centre of gravity of mass m_1 —the x -axis of which coincides with the line joining the centres of the two stars (i.e., the radius-vector of the relative orbit of the two masses which will—in this chapter—be regarded as constant); while the z -axis is perpendicular to the plane of the orbit. If so, the coordinates of the centre of gravity of the system are

$$\frac{m_2 R}{m_1 + m_2}, 0, 0; \quad (1.1)$$

and the total potential Ψ of all forces acting at an arbitrary point $P(x, y, z)$ becomes expressible as

$$\Psi = G \frac{m_1}{r} + G \frac{m_2}{r'} + \frac{\omega^2}{2} \left\{ \left(x - \frac{m_2 R}{m_1 + m_2} \right)^2 + y^2 \right\} \quad (1.2)$$

where

$$r^2 = x^2 + y^2 + z^2; \quad r'^2 = (R - x)^2 + y^2 + z^2, \quad (1.3)$$

represent squares of the distance of P from the centres of gravity of the two components, and ω denotes the angular velocity of rotation of the system about an axis perpendicular to the orbital plane and passing through the centre of gravity of the system whose coordinates are given by (1.1). The first term on the right-hand side of Equation (1.2) represents the potential arising from the mass m_1 ; the second, the disturbing potential of its companion of mass m_2 ; and the third, the potential arising from the centrifugal force.

Let, furthermore, the angular velocity ω on the right-hand side of Equation (1.2) be identified with the Keplerian angular velocity

$$\omega^2 = \frac{G(m_1 + m_2)}{R^3} \quad (1.4)$$

of the system. If we insert (1.4) in (1.2) and, moreover, adopt m_1 as our unit of mass; R , as the unit of length while the unit of time is chosen so that $G = 1$, Equation (1.2) may be expressed in terms of spherical polar coordinates

$$\left. \begin{aligned} x &= r \cos \phi \sin \theta = r \lambda, \\ y &= r \sin \phi \sin \theta = r \mu, \\ z &= r \cos \theta = r \nu, \end{aligned} \right\} \quad (1.5)$$

as

$$\xi = \frac{1}{r} + q \left\{ \frac{1}{\sqrt{1 - 2\lambda r + r^2}} - \lambda r \right\} + \frac{q+1}{2} r^2 (1 - \nu^2), \quad (1.6)$$

where

$$\xi \equiv \frac{R\Psi}{Gm_1} - \frac{m_2^2}{2m_1(m_1 + m_2)} \quad (1.7)$$

and

$$q \equiv \frac{m_2}{m_1} \quad (1.8)$$

the two masses $m_{1,2}$ (and, therefore, their ratio q being likewise regarded as constant).

Within the scheme of definitions adopted, none of the terms constituting the normalized potential ξ depends on the time; and Equation (1.6) defining it will generate surfaces described by the polar coordinates r, λ, ν ; the forms of which are governed by the non-dimensional values of ξ and q . If ξ is large, the corresponding surfaces—hereafter referred to as the *Roche Equipotentials*—will consist of two separate ovals (see Figure II.1) closed around each of the two mass-points; for the right-hand side of (1.6) can be large only if r (or $r' = \sqrt{1 - 2\lambda r + r^2}$) becomes small; and if the left-hand side of (1.6) is to be constant, so must be (very nearly) r or r' . Large values of ξ correspond, therefore, to equipotentials differing but little from spheres—the less so, the greater ξ becomes. With diminishing value

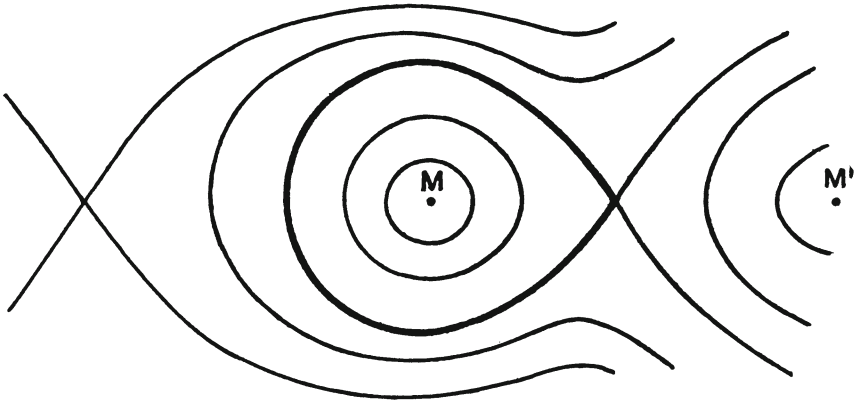


Figure II.1: A cross-section of the Roche Model of a binary system of masses m and m' ; the heavy line representing the Roche limit (after Jeans, 1919).

of ξ the ovals defined by (1.6) become increasingly elongated in the direction of the centre of gravity of the system — until, for a certain critical value of ξ_1 characteristic of each mass-ratio, both ovals will unite in a single point on the x -axis to form a dumb-bell-like configuration (cf. again Figure II.1) which we propose to call the *Roche Limit*.¹ For still smaller values of ξ the connecting part of the dumb-bell opens up and the corresponding equipotential surfaces would envelop both bodies. This latter case is, however, of no direct interest to us in this connection; as for $\xi < \xi_1$ the two initially distinct bodies would coalesce in one and we should no longer have the right to speak of a binary system. In what follows we shall, therefore, limit ourselves to a study of the geometry of surfaces characterized by $\xi \geq \xi_1$.

II.2 Geometry of Roche Equipotentials

Equation (1.6) of the Roche equipotentials represents an implicit function defining, for given values of ξ and q, r as a function of λ and ν . When it has been rationalized and cleared of fractions, the result is an algebraic equation of *eighth* degree in r , whose analytical solution presents unsurmountable difficulties. In

¹Not to be confused with a concept used, under the same name, in other literature to signify the minimum distance to which a fluid satellite of infinitesimal mass can approach with impunity an oblate planet. This latter term, coined in the latter half of the 19th century by G. H. Darwin, has nothing to do with the “Roche Limit” as defined in this section (and introduced under this name by Kopal (1955) to describe the fractional size of “contact” components in semi-detached eclipsing systems).

the case of pure rotational distortion (obtaining if $q = 0$) Equation (1.6) can be reduced to a cubic solvable in terms of circular functions. In the case of a purely tidal distortion ($\omega = 0$), Equation (1.6) becomes a quartic, which could also be solved for r in a closed form (though its solution would be very much more involved). However, in the general case of rotational *and* tidal distortion interacting, any attempt at an *exact* solution of (1.6) for r becomes virtually hopeless; and approximate solutions must be sought by successive approximations.

A: Radius and Volume

In order to obtain them, let us begin by expanding the radical $(1 - 2\lambda r + r^2)^{-1/2}$ on the right-hand side of (1.6) in terms of the Legendre polynomials $P_j(\lambda)$. Doing so and removing fractions we find it possible to replace (1.6) by

$$(\xi - q)r = 1 + q \sum_{j=2}^{\infty} r^{j+1} P_j(\lambda) + nr^3(1 - \nu^2), \quad (2.1)$$

where we have abbreviated

$$n = \frac{q + 1}{2} \quad (2.2)$$

If r is small in comparison with unity (i.e., if the linear dimensions of the equipotential surfaces are small in comparison with our unit of length R), the second and third terms on the right-hand side of (2.1) may be neglected in comparison with unity—in which case

$$r_0 = \frac{1}{\xi - q}. \quad (2.3)$$

This result asserts that if ξ is large, the corresponding Roche equipotential will differ but little from a sphere of radius r_0 .

Suppose now that

$$r_1 = r_0 + \Delta' r = r_0 \left(1 + \frac{\Delta' r}{r_0} \right) \quad (2.4)$$

should represent our next approximation to r . Inserting it in (2.1) we find that

$$1 + \frac{\Delta' r}{r_0} = 1 + q \sum_{j=2}^{\infty} r_0^{j+1} P_j(\lambda) + nr_0^3(1 - \nu^2) \quad (2.5)$$

where, in small terms on the right-hand side, r was legitimately replaced by r_0 . The foregoing equation then yields

$$\frac{\Delta' r}{r_0} = q \sum_{j=2}^4 r_0^j P_j(\lambda) + nr_0^3(1 - \nu^2) \quad (2.6)$$

correctly to quantities of the order of r_0^5 (i.e., as far as squares and higher terms of first-order distortion remain negligible).

In order to improve upon this approximation let us set, successively,

$$r_2 = r_1 + \Delta''r = r_0 \left\{ 1 + \frac{\Delta'r}{r_0} + \frac{\Delta''r}{r_0} \right\}, \quad (2.7)$$

$$\begin{aligned} r_3 &= r_2 + \Delta'''r = r_0 \left\{ 1 + \frac{\Delta'r}{r_0} + \frac{\Delta''r}{r_0} + \frac{\Delta'''r}{r_0} \right\} \\ &\quad \vdots \quad \quad \quad \vdots \end{aligned} \quad (2.8)$$

$$r_{j+1} = r_j + \Delta^{(j+1)}r = r_0 \left\{ 1 + \sum_{i=0}^j \frac{\Delta^{(i+1)}r}{r_0} \right\}, \quad (2.9)$$

where

$$\frac{\Delta^{(i+1)}r}{r_0} = q \sum_{k=3}^{3(N-i)} (r_i^k - r_{i-1}^k) P_{k-1}(\lambda) + n(r_i^3 - r_{i-1}^3)(1 - \nu^2); \quad (2.10)$$

$3N$ denoting the highest power of r_0 to which Equation (2.9) represents a correct solution for r . We may note that, in general, the leading terms of the expression (2.10) for $\Delta^{(i+1)}r/r_0$ will be of $3(i+1)$ st degree in r_0 ; and, similarly, the difference $r_i^k - r_{i-1}^k$ in higher terms on the right-hand side of (2.10) will be of the order of r_0^{3i+k} .

Suppose that, in what follows, we wish to construct the explicit form of an approximate solution of Equation (2.1), in the form of (2.8), correctly to (say) quantities of the order of $\Delta'''r/r_0$ —which should, therefore, differ from the exact solution of (2.1) at most in quantities of the order of r_0^{12} . By use of the expression already established for $\Delta'r/r_0$ the explicit forms of $\Delta''r/r_0$ and $\Delta'''r/r_0$ can successively be found² and their insertion in (2.8) leads to the equation

$$\begin{aligned} \frac{r - r_0}{r_0} &= r_0^3 \{qP_2 + n(1 - \nu^2)\} + r_0^4 \{qP_3\} + r_0^5 \{qP_4\} + \\ &\quad + r_0^6 \{qP_5 + 3[qP_2 + n(1 - \nu^2)]^2\} + \\ &\quad + r_0^7 \{qP_6 + 7q[qP_2 + n(1 - \nu^2)]P_3\} + \\ &\quad + r_0^8 \{qP_7 + 8q[qP_2 + n(1 - \nu^2)]P_4 + 4q^2P_3^2\} + \\ &\quad + r_0^9 \{qP_8 + 9q[qP_2 + n(1 - \nu^2)]P_5 + 9q^2P_3P_4 + \\ &\quad \quad + 6[qP_2 + n(1 - \nu^2)]^3 + 6[q^3P_2^3 + n^3(1 - \nu^2)^3]\} + \\ &\quad + r_0^{10} \{qP_9 + 10q[qP_2 + n(1 - \nu^2)]P_6 + 5q^2[P_4^2 + 2P_3P_5] + \\ &\quad \quad + 45q[qP_2 + n(1 - \nu^2)]^2P_3\} + \\ &\quad + r_0^{11} \{qP_{10} + 11q([qP_2 + n(1 - \nu^2)]P_7 + 11q^2[P_3P_6 + P_4P_5] + \\ &\quad \quad + 55q[qP_2 + n(1 - \nu^2)]^2P_4 + \\ &\quad \quad + 55q^2[qP_2 + n(1 - \nu^2)]P_3^2\} + \dots, \end{aligned} \quad (2.11)$$

² For fuller details of this process, cf. Kopal (1954, 1959).

where we have abbreviated $P_j \equiv P_j(\lambda)$, and which represents the desired approximate solution of Equation (2.1) for r as a function of λ and ν in the form of an expansion in ascending powers of r_0 (as defined by Equation (2.3)).

The volume V of a configuration whose radius-vector r is given by the foregoing Equation (2.12) will be specified by

$$V = \frac{2}{3} \int_{-1}^1 \int_{-\sqrt{1-\lambda^2}}^{\sqrt{1-\lambda^2}} \frac{r^3 d\lambda d\nu}{\mu}, \quad (2.12)$$

where $\mu^2 = 1 - \lambda^2 - \nu^2$. By virtue of the algebraic identity

$$r^3 = r_0^3 \left\{ 1 + \frac{r - r_0}{r_0} \right\}^3 \quad (2.13)$$

we find it convenient to express the integrand in (2.12) in terms of (2.13) as a function of λ and ν . This integrand will, in general, consist of a series of terms of the form $\lambda^m \nu^n / \mu$, factored by constant coefficients; therefore, the entire volume V will be given by an appropriate sum of partial expressions V_n^m of the form

$$V_n^m = \int_{-1}^1 \int_{-\sqrt{1-\lambda^2}}^{\sqrt{1-\lambda^2}} \frac{\lambda^m \nu^n}{\mu} d\lambda d\nu. \quad (2.14)$$

These expressions vanish (on grounds of symmetry) if either m or n is an odd integer. If, however, both happen to be even and such that $m = 2a$ and $n = 2b$, an evaluation of the foregoing integrals readily reveals that

$$V_{2b}^{2a} = \frac{\sqrt{\pi} \Gamma(a + \frac{1}{2}) \Gamma(b + \frac{1}{2})}{\Gamma(a + b + \frac{3}{2})}, \quad (2.15)$$

where Γ denotes the ordinary gamma function. As, accordingly,

$$\int_{-1}^1 \int_{-\sqrt{1-\lambda^2}}^{\sqrt{1-\lambda^2}} \frac{P_j(\lambda) d\lambda d\nu}{\sqrt{1-\lambda^2-\nu^2}} = \begin{cases} 2\pi & \text{if } j = 0 \\ 0 & \text{if } j > 0 \end{cases} \quad (2.16)$$

and

$$\int_{-1}^1 \int_{-\sqrt{1-\lambda^2}}^{\sqrt{1-\lambda^2}} \frac{\nu^{2j} d\lambda d\nu}{\sqrt{1-\lambda^2-\nu^2}} = \frac{2\pi}{j+1}, \quad (2.17)$$

we eventually find that the volume of a configuration whose surface is a Roche equipotential will be given by

$$\begin{aligned} V = & \frac{4}{3} \pi r_0^3 \left\{ 1 + \frac{12}{5} q^2 r_0^6 + \frac{15}{7} q^2 r_0^8 + \frac{18}{9} q^2 r_0^{10} + \dots \right. \\ & + \frac{22}{7} q^3 r_0^9 + \frac{157}{7} q^3 r_0^{11} + 2n r_0^3 + \frac{32}{5} n^2 r_0^6 + \frac{176}{7} n^3 r_0^9 + \dots \\ & \left. + \frac{8}{5} n q r_0^6 + \frac{296}{35} n q (2q + n) r_0^9 + \frac{26}{35} n q (q + 3n) r_0^{11} + \dots \right\}, \quad (2.18) \end{aligned}$$

correctly to quantities of the order up to and including r_0^{11} . With n and r_0 as given by Equations (2.2) and (2.3) the volume V becomes an explicit function of ξ and q alone and can be tabulated in terms of these parameters.

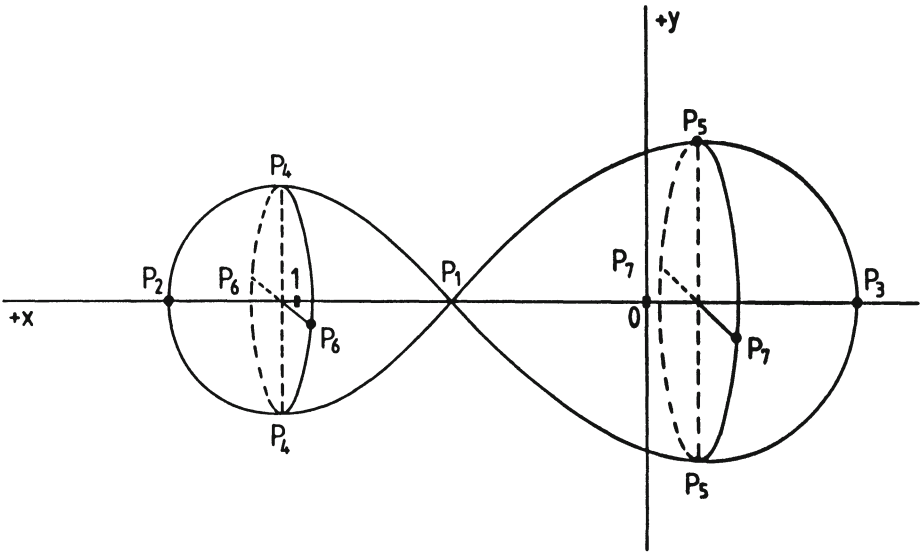


Figure II.2: Schematic view of a contact binary at the Roche Limit. In order to exhibit the essential features of the geometry of this model, the diagram has not been drawn to scale for any particular mass-ratio; and certain features of it (such as the distance of the P_5P_7 -plane from the origin) have been exaggerated.

B: Roche Limit

It was pointed out already in Section II.1 that a diminution of the value of the constant ξ on the left-hand side of Equation (1.6) will cause the respective Roche equipotentials to expand from nearly spherical configurations to ovals of increased elongation in the direction of the attracting centre until, for a certain critical value of ξ characteristic of each mass-ratio, these ovals unite in a single point on the line joining their centres. Such configurations represent the largest *closed* equipotentials capable of containing the whole mass of the respective components, and will hereafter be referred to as their *Roche limits*. Any star filling its Roche limit will therefore be termed a *contact component*; and a binary system consisting of a pair of such components, a *contact system*. The fact that close binaries in which one, or both, components have attained their Roche limits actually exist in considerable numbers in the sky underlines the importance of a study of the geometry of Roche limits in binary systems of different mass-ratios.

In order to do so, our first task should be to specify the values of ξ for which the two loops of the critical equipotential (cf. Figure II.2) develop a common point of contact at P_1 ; but its determination presupposes a knowledge of the position of P_1 on the x -axis. The location of this point is characterized by the vanishing of the gravity due to all forces - which means that, at that point,

$$\xi_x = \xi_y = 0 . \quad (2.19)$$

Now a differentiation of (1.6), rewritten in terms of rectangular coordinates, with respect to x and y yields

$$\xi_x = -xr^{-3} + q\{(1-x)(r')^{-3} - 1\} + 2nx , \quad (2.20)$$

$$\xi_y = -y\{r^{-3} + q(r')^{-3} - 2n\} , \quad (2.21)$$

$$\xi_z = -zr^{-3} - qz(r')^{-3} , \quad (2.22)$$

where $r^2 = x^2 + y^2 + z^2$ and $r'^2 = (1-x)^2 + y^2 + z^2$ continue to be given by Equations (1.3) and $2n = q + 1$ in accordance with (2.2).

The partial derivative ξ_y vanishes evidently everywhere along the x -axis; but the vanishing of ξ_x renders the x -coordinate of P_1 to be a root of the equation

$$x^{-2} - x = q\{(1-x)^{-2} - (1-x)\} \quad (2.23)$$

which, after removal of the fractions, assumes the form

$$(1+q)x^5 - (2+3q)x^4 + (1+3q)x^3 - x^2 + 2x - 1 = 0 . \quad (2.24)$$

For $q = 0$ the foregoing equation would evidently reduce to

$$(1-x)^3(x^2+x+1) = 0 , \quad (2.25)$$

the value $x = 1$ becoming a triple root. Therefore, for small values of q , the root x_1 of Equation (2.23) which is interior to the interval $0 < x < 1$ can be approximated by the expansion

$$x_1 = 1 - w + \frac{1}{3}w^2 + \frac{1}{9}w^3 + \dots \quad (2.26)$$

in terms of the auxiliary parameter

$$w^3 = \frac{1}{3(1+q)} ; \quad (2.27)$$

and more accurate values of x_1 can further be obtained by the method of differential corrections.

Once a sufficiently accurate value of x_1 has thus been obtained, the actual value of ξ corresponding to our critical equipotential follows as

$$\xi_1 \equiv \xi(x_1, 0, 0) . \quad (2.28)$$

Moreover, the points $P_{4,5}$ in the xy -plane (see again Figure II.2) are evidently characterized by the vanishing of the derivative dy/dx at the Roche limit. Their coordinates $x_{4,5}$ and $y_{4,5}$ can, therefore, be evaluated by solving the simultaneous system

$$\left. \begin{aligned} \xi(x, y, 0) &= \xi_1 , \\ \xi_x(x, y, 0) &= 0 ; \end{aligned} \right\} \quad (2.29)$$

q	x_1	ξ_1	x_4	$\pm y_4$	x_5	$\pm y_5$	$\pm z_6$	$\pm z_7$
1.0	0.50000	3.75000	1.01134	0.37420	-0.01134	0.37420	0.35621	0.35621
0.8	0.52295	3.41697	1.01092	0.35388	-0.01168	0.39501	0.33770	0.37491
0.6	0.55234	3.06344	1.01029	0.32853	-0.01198	0.42244	0.31431	0.39909
0.4	0.59295	2.67810	1.00926	0.29465	-0.01213	0.46189	0.28260	0.43278
0.3	0.62087	2.46622	1.00847	0.27204	-0.01204	0.49015	0.26123	0.45599
0.2	0.65856	2.23273	1.00735	0.24233	-0.01163	0.52989	0.23294	0.48714
0.15	0.68392	2.10309	1.00656	0.22280	-0.01117	0.55774	0.21425	0.50781
0.1	0.71751	1.95910	1.00552	0.19746	-0.01034	0.59609	0.18991	0.53451
0.05	0.76875	1.78886	1.00397	0.15979	-0.00859	0.65804	0.15366	0.57291
0.02	0.82456	1.65702	1.00245	0.11992	-0.00618	0.73070	0.11522	0.61434
0.01	0.85853	1.59911	1.00165	0.09613	-0.00457	0.77779	0.09231	0.62867
0.005	0.88635	1.56256	1.00110	0.07689	-0.00327	0.81807	0.07379	0.64170
0.001	0.93231	1.52148	1.00041	0.04550	-0.00137	0.88816	0.04361	0.65762
0.0002	0.96001	1.50737	1.00015	0.02678	-0.00052	0.93264	0.02566	0.66348
0	1.00000	1.50000	1.00000	0.00000	0.00000	1.00000	0.00000	0.66667

Table II.1:

and once the values of $x_{4,5}$ have thus been found, the z -coordinates of points $P_{6,7}$ in the xz -plane (cf. Figure II.2) follow as roots of a single equation

$$\xi(x_{4,5}, 0, z) = \xi_1 . \tag{2.30}$$

The accompanying Table II.1 lists five-digit values of $\xi_1, x_1; x_{4,5}, y_{4,5}$; and $z_{6,7}$ for Roche limits appropriate for 15 discrete values of the mass-ratio.

It may further be noted that if, in place of ξ_1 , we introduce a new constant C_1 as defined by the equation

$$C_1 = \frac{2\xi_1}{1+q} + \left(\frac{q}{1+q}\right)^2 = 2(1-\mu)\xi_1 + \mu^2 , \tag{2.31}$$

where we have abbreviated

$$\mu = \frac{q}{1+q} = \frac{m_2}{m_1+m_2}, \quad 1-\mu = \frac{1}{1+q} = \frac{m_1}{m_1+m_2} , \tag{2.32}$$

the values of C_1 remain largely invariant with respect to the mass-ratio, and sensibly equal to 4 provided that q does not depart greatly from unity. This is demonstrated by an inspection of the tabulation of C_1 as given in column (2) of the following Table II.2. In consequence, the simple expression

$$\xi_1 \doteq 2(1+q) - \frac{q^2}{2(1+q)} = \frac{4-\mu^2}{2(1-\mu)} \tag{2.33}$$

q	C_1	$(r_0)_1$	$(r_0)_2$	V_1	V_2	$(r^*)_1$	$(r^*)_2$	v_1	v_2
1	4.00000	0.36363	0.36363	0.22704	0.22704	0.37845	0.37845	0.072267	0.072267
0.8	3.99417	0.38212	0.34528	0.26459	0.19374	0.39825	0.35896	0.075799	0.069377
0.6	3.96993	0.40594	0.32199	0.31974	0.15665	0.42420	0.33441	0.081422	0.066485
0.4	3.90749	0.43896	0.29025	0.40923	0.11444	0.46057	0.30115	0.091184	0.063726
0.3	3.84744	0.46163	0.26876	0.48148	0.09089	0.48622	0.27892	0.099619	0.062683
0.2	3.74900	0.49195	0.24018	0.59399	0.06492	0.52147	0.24933	0.113443	0.061996
0.15	3.67456	0.51201	0.22121	0.68002	0.05079	0.54552	0.22973	0.124462	0.061967
0.1	3.57027	0.53789	0.19642	0.80715	0.03564	0.57760	0.20414	0.141308	0.062385
0.05	3.40962	0.57509	0.15931	1.0289	0.01910	0.62626	0.16584	0.17193	0.063854
0.02	3.24945	0.61087	0.11974	1.2700	0.007961	0.67179	0.12387	0.2062	0.06462
0.01	3.16665	0.62928	0.09606	1.4656	0.004042	0.70465	0.09882	0.2356	0.06497
0.005	3.10959	0.64203	0.07686	1.5950	0.002038	0.7248	0.07865	0.2551	0.06520
0.001	3.03992	0.65769	0.04549	1.868	0.0004114	0.764	0.04614	0.298	0.06554
0.0002	3.01414	0.66350	0.02679	2.067	0.0000826	0.790	0.02702	0.329	0.06575
0	3.00000	0.66667	0.00000	2.26663	0.0000000	0.81488	0.00000	0.36075	0.065843

Table II.2: The data collected in Tables II.1 and 2 are taken from Kopal (1959). More extensive tabulations of the same parameters for $q = 1(-0.02)$ 0.10 to $5D$ have since been prepared by Plavec and Kratochvíl (1964). Cf. also ten Bruggencate (1934).

is found to approximate the exact values of ξ_1 within 1% if $1 \geq q \geq 0.5$, or within 10% for the wider range $1 \geq q \geq 0.1$. The mean radii $(r_0)_{1,2}$ of the two components of contact systems become (consistent with Equations (2.3) and (2.31)) equal to

$$(r_0)_{1,2} = \frac{2(1-\mu)}{C_1 - (1+\mu)^2 + 1} \quad (2.34)$$

where, for the primary component, $0 \leq \mu \leq 0.5$; while, for the secondary, $0.5 \leq \mu \leq 1$. Alternatively, we may fall back on Equation (2.3) and, by inserting for ξ_1 from (2.28) write

$$(r_0)_1 = \frac{2x_1}{2 + 2qx_1^3(1-x_1)^{-1} + (q+1)x_1^3}; \quad (2.35)$$

while $(r_0)_2$ is obtainable from the same expression if we replace x_1 by $1-x_1$ and q by its reciprocal. The values of $(r_0)_{1,2}$ so determined are listed as functions of the mass-ratio in columns (3) and (4) of Table II.2.

Having evaluated them, we are in a position to invoke Equation (2.19) for expressing the volumes $V_{1,2}$ of contact components—the reader will find them tabulated in columns (5) and (6) of Table II.2—while columns (7) and (8) list the equivalent radii $(r^*)_{1,2}$ of spheres having the same volume as the respective contact component. The penultimate and ultimate columns of Table II.2 then

contain the quantities

$$v_{1,2} = \frac{\omega^2}{2\pi G \bar{\rho}_{1,2}} = \frac{2}{3} \left\{ 1 + \frac{m_{2,1}}{m_{1,2}} \right\} (r^*)_{1,2}^3, \quad (2.36)$$

where ω denotes the (Keplerian) angular velocity of axial rotation of each component and $\bar{\rho}_{1,2}$, their respective mean densities.

The series on the right-hand side of the volume equation (2.19)—which are at the basis of our numerical data as given in columns (5)–(10)—converge with satisfactory rapidity if the masses of the two components are not too unequal, but fail to do so if the mass of one component becomes very much larger than the other. In order to attain adequate representation of the radii and volumes in such cases, asymptotic solutions of Equation (2.1) must be sought as $\mu \rightarrow 0$ or 1.

In order to do so, we find it advantageous to rewrite (1.6) in the alternative form

$$(1 - 2\lambda r + r^2)\{(1 - \nu^2)r^3 - 2\lambda\mu r^2 + (\mu^2 - C_1)r + 2(1 - \mu)\}^2 = 4\mu^2 r^2, \quad (2.37)$$

where C_1 as well as μ are defined by Equations (2.31) and (2.32); and consider first the case of very small disturbing mass (when $\mu \rightarrow 0$). As long as quantities of the order of μ^2 remain ignorable, Equation (2.37) will admit of a real solution only if

$$(1 - \nu^2)r^3 - 2\lambda\mu r^2 - C_1 r + 2(1 - \mu) = 0. \quad (2.38)$$

For small values of μ , the solution of this latter equation can be sought in the form

$$r = S_{10} + S_{11}\mu + \dots, \quad (2.39)$$

where S_{10}, S_{11}, \dots are defined by the equations

$$(1 - \nu^2)S_{10}^3 - C_1 S_{10} + 2 = 0, \quad (2.40)$$

$$3(1 - \nu^2)S_{10}^2 S_{11} - C_1 S_{11} - 2 = 2\lambda S_{10}^2, \quad (2.41)$$

etc., whose solutions become

$$S_{10} = 2 \left\{ \frac{C_1}{3(1 - \nu^2)} \right\}^{1/2} \sin \left\{ \frac{1}{3} \sin^{-1} \frac{3}{C_1} \sqrt{\frac{3(1 - \nu^2)}{C_1}} \right\} \quad (2.42)$$

and

$$S_{11} = \frac{2(1 + \lambda S_{10}^2)}{3(1 - \nu^2)S_{10}^2 - C_1}, \quad (2.43)$$

respectively

Equation (2.39) with its coefficients as given by (2.42) and (2.43) will closely approximate the form of the primary component of a contact system which is very much more massive than the secondary. Its first term S_{10} defines obviously the form of a Roche equipotential distorted by centrifugal force alone. If $\mu \rightarrow 0$, $\xi_1 \rightarrow$

1.5 and $C_1 \rightarrow 3$, in which case the parametric equation of the corresponding critical equipotential assumes the neat form

$$r = \frac{2}{\sqrt{1-\nu^2}} \left\{ \sin \frac{1}{3} \cos^{-1} \nu \right\} = 2 \frac{\sin \frac{1}{3} \theta}{\sin \theta}; \quad (2.44)$$

and its volume V_1 , in accordance with Equation (2.12), becomes

$$\begin{aligned} V_1 &= \frac{32}{3} \pi \int_0^1 (1-\nu^2)^{-3/2} \sin^3 \left(\frac{1}{3} \cos^{-1} \nu \right) d\nu = \\ &= \frac{4}{3} \pi \left\{ 3\sqrt{3} - 4 + 3 \log \frac{3(\sqrt{3}-1)}{\sqrt{3}+1} \right\} = 2.26662 \dots, \end{aligned} \quad (2.45)$$

so that, by (2.36), $v_1 \equiv V_1/2\pi = 0.36074$. It is the foregoing values, rather than those which would follow from a straightforward application of (2.19), which have been used to complete the last entries in columns (5) and (9) of Table II.2.

If the primary component accounts thus for most part of the total mass of our contact binary system, the volume of the secondary must clearly tend to zero. The form of its surface will, in turn, be given by an asymptotic solution of Equation (2.37) as $\mu \rightarrow 1$. Let us, therefore, expand this solution in a series of the form

$$r = S_{20}(1-\mu) + S_{21}(1-\mu^2) + \dots; \quad (2.46)$$

inserting it in (2.37) we find the vanishing of the coefficients of equal powers of $(1-\mu)$ to require that

$$S_{20} = \frac{2}{C_1-3}, \quad S_{21} = - \left\{ 2 + \frac{\lambda}{C_1-3} \right\} S_{20}^2, \quad (2.47)$$

etc.. An application of Equation (2.12) reveals, moreover, that the volume V_2 of the respective configuration should be approximable by

$$V_2 = \frac{4}{3} \pi \{ (1-\mu)^3 S_{20}^3 - 6(1-\mu)^4 S_{20}^4 - \dots \}, \quad (2.48)$$

and the radius r_2^* of a sphere of equal volume becomes

$$r_2^* = (1-\mu)S_{20} - 2(1-\mu)^2 S_{20}^2 + \dots \quad (2.49)$$

A glance at the second column of Table II.2 reveals that, as $q \rightarrow 0$, $C_1 \rightarrow 3$ and, as a result the product $(1-\mu)S_{20}$ tends to become indeterminate for $\mu = 1$. In order to ascertain its limiting value, let us depart from Equation (2.31) which, on insertion of ξ_1 from (2.28) assumes the form

$$C_1 = \frac{2(1-\mu)}{1-x_1} + \frac{2\mu}{x_1} + (1-\mu-x_1)^2, \quad (2.50)$$

with the root x_1 approximable by means of (2.26) where, by (2.27) and (2.32),

$$3w^3 = 1-\mu. \quad (2.51)$$

Inserting (2.26) in (2.50) we find that, within the scheme of our approximation,

$$C_1 = 3(1 + 3w^2 - 4w^3 + \dots); \quad (2.52)$$

so that

$$(1 - \mu)S_{20} = \frac{2w}{3 - 4w} + \dots, \quad (2.53)$$

and therefore

$$r_2^* = \frac{2}{3}w - \frac{32}{27}w^3 + \dots. \quad (2.54)$$

In consequence, it follows from (2.36) that, for a secondary component of vanishing mass

$$v_2 = \frac{1}{3} \left(\frac{2}{3} \right)^4 \left\{ 1 - \frac{16}{3}w^2 + \dots \right\}. \quad (2.55)$$

An inspection of the last two columns of Table II.2 reveals that, for the primary (more massive) component, the value of v_1 increases monotonously with diminishing mass-ratio m_2/m_1 from 0.07227 for the case of equality of masses to 0.36075 for $m_2 = 0$, at which point the primary component becomes rotationally unstable and matter begins to be shed off along the equator if axial rotation is any faster. On the other hand, for the secondary (less massive) component the values of v_2 diminish with decreasing mass-ratio from 0.07227 until, as $m_2 \rightarrow 0$, the value of $2^4/3^5$ has been attained.

C: Geometry of the Eclipses

The data assembled in the foregoing section on the geometry of contact configurations lead to a number of specific conclusions regarding the eclipse phenomena to be exhibited by such systems. For suppose that a contact binary both of the components of which are at their Roche limits is viewed by a distant observer, whose line of sight does not deviate greatly from the x -axis of our model as shown on Figure II.2 If so, then in the neighbourhood of either conjunction one component is going to eclipse the other, and the system will exhibit a characteristic variation in brightness. if, in turn, the observed light variation is analyzed for the geometrical elements the fractional "radii" $r_{1,2}$ of the two components should (very approximately) be identical with the quantities $y_{4,5}$ as listed in columns (5) and (7) of Table II.2. In Table II.3 we have, accordingly, listed four-digit values of the sums $r_1 + r_2$ as well as the ratios r_2/r_1 of the "radii" of such contact components as functions of their mass-ratio.

An inspection of this tabulation reveals that, within the scheme of our approximation, *the sum $r_1 = r_2$ of fractional radii of both components in contact binary systems is very nearly constant* and equal to 0.75 ± 0.01 for a very wide range of the mass-ratios q ; whereas the *ratio r_2/r_1 decreases monotonically with diminishing value of q* . Therefore, a photometric determination of the sum $r_1 + r_2$ — which, unfortunately, represents nearly all that can be deduced with any accuracy from an analysis of light curves due to shallow partial eclipses — cannot

q	$r_1 + r_2$	r_1/r_2
1.0	0.7474	1.0000
0.9	0.7486	0.9495
0.8	0.7489	0.8959
0.7	0.7496	0.8389
0.6	0.7510	0.7777
0.5	0.7529	0.7112
0.4	0.7565	0.6379
0.3	0.7622	0.5550
0.2	0.7722	0.4573
0.15	0.7805	0.3995
0.1	0.7935	0.3312

Table II.3:

be expected to tell us anything new about contact systems; or, in particular, about their mass-ratios. It is the ratio of the radii r_2/r_1 whose determination would provide a sensitive photometric clue to the mass-ratio of a contact system. This underlines the importance of photometric determination of the ratios of the radii of contact binary systems; but owing to purely geometrical difficulties this important task of light curve analysis is, unfortunately, not yet well in hand.

Suppose next that a contact binary system, consisting of two components at their Roche limits, is viewed by a distant observer from an arbitrary direction. What will be the range of such directions from which this observer will see both bodies mutually eclipse each other during their revolution? In order to answer this question, let us replace the actual form of the corresponding Roche limit by an *osculating cone* which is tangent to it at the point of contact P_1 . The equation of this cone may readily be obtained if we expand the function $\xi(x, y, z)$ of Roche equipotentials in a Taylor series, in three variables, about P_1 .

The first partial derivatives ξ_x , ξ_y and ξ_z have already been given by Equations (2.20)–(2.22) in the preceding part of this section. Differentiating these equations further we find that

$$\xi_{xx} = (3x^2 - r^2)r^{-5} + q\{3(1-x)^2 - r'^2\}(r')^{-5} + q + 1, \quad (2.56)$$

$$\xi_{yy} = (3y^2 - r^2)r^{-5} + q\{3y^2 - r'^2\}(r')^{-5} + q + 1, \quad (2.57)$$

$$\xi_{zz} = (3z^2 - r^2)r^{-5} + q\{3z^2 - r'^2\}(r')^{-5}, \quad (2.58)$$

$$\xi_{xy} = 3xyr^{-5} - 3q(1-x)y(r')^{-5}, \quad (2.59)$$

$$\xi_{xz} = 3xzr^{-5} - 3q(1-x)z(r')^{-5}, \quad (2.60)$$

$$\xi_{yz} = 3yzt^{-5} + 3qyz(r')^{-5}. \quad (2.61)$$

We note that all first (as well as mixed second) derivatives of ξ vanish at P_1 . Hence, a requirement that the sum of nonvanishing second-order terms should add up to zero provides us with the desired equation of the osculating cone in the form

$$(x - x_1)^2(\xi_{xx})_1 + y^2(\xi_{yy})_1 + z^2(\xi_{zz})_1 = 0, \quad (2.62)$$

where

$$\begin{aligned} (\xi_{xx})_1 &= 2p + q + 1, \\ (\xi_{yy})_1 &= -p + q + 1, \\ (\xi_{zz})_1 &= -p, \end{aligned} \quad (2.63)$$

in which we have abbreviated

$$p \equiv x_1^{-3} + q(1 - x_1)^{-3}. \quad (2.64)$$

The direction cosines l, m, n , of a line normal to the surface of this cone clearly are given by

$$l, m, n = \{f_\xi, f_y, f_z\} \div \{f_\xi^2 + f_y^2 + f_z^2\}^{1/2}, \quad (2.65)$$

where $f(\zeta, y, z)$ stands for the left-hand side of Equation (2.62) and $\zeta \equiv x - x_1$. Moreover, the direction cosines of the axis of this cone in the same coordinate system are $(1, 0, 0)$. Consequently, the angle ϵ between any arbitrary line on the surface of the osculating cone and its axis will be defined by the equation

$$l = \cos\left(\frac{1}{2}\pi - \epsilon\right) = \sin \epsilon; \quad (2.66)$$

so that

$$\tan^2 \epsilon = \frac{l^2}{1 - l^2} = \frac{f_\zeta^2}{f_y^2 + f_z^2}; \quad (2.67)$$

where, by (2.62),

$$f \equiv \zeta^2(\xi_{xx})_1 + y^2(\xi_{yy})_1 + z^2(\xi_{zz})_1 = 0. \quad (2.68)$$

Therefore,

$$\frac{f_\zeta^2}{f_y^2 + f_z^2} = \frac{[\zeta(\xi_{xx})_1 y]^2}{[(\xi_{yy})_1 y]^2 + [(\xi_{zz})_1 z]^2}. \quad (2.69)$$

Since, moreover, it follows from Equation (2.62) that $\zeta^2(\xi_{xx})_1 = -y^2(\xi_{yy})_1 - z^2(\xi_{zz})_1$, it follows on insertion in (2.67) that

$$\begin{aligned} \tan^2 \epsilon &= - \left\{ \frac{(\xi_{yy})_1 y^2 + (\xi_{zz})_1 z^2}{(\xi_{yy})_1^2 y^2 + (\xi_{zz})_1^2 z^2} \right\} (\xi_{xx})_1 = \\ &= \left\{ \frac{(p - q - 1)y^2 + pz^2}{(p - q - 1)^2 y^2 + p^2 z^2} \right\} (2p + q + 1), \end{aligned} \quad (2.70)$$

where the values of $\xi_{xx}, \xi_{yy}, \xi_{zz}$ at the conical point P of Figure II.2 are given by Equations (2.64).

All the foregoing results of this section have been based on the approximation of the Roche lobes in contact by an osculating cone at P_1 . While this should always constitute a legitimate basis for computations of the limits of eclipses by the less massive component of a contact pair (in the sense that its surface is always interior to the common osculating cone), Chanan *et al* (1976) called attention recently to the fact that the surface of the more massive component can actually "overflow" this cone by amounts increasing with the disparity in masses of the two stars.

In order to demonstrate this, let us expand—in accordance with Equation (1.2)—the Roche equipotentials $\Psi(x, y, z)$ of a contact loop in the proximity of the point P_1 of coordinates $x_1, 0, 0$ in a Taylor series of the form

$$\begin{aligned} \Psi(x_1, y, z) = & \Psi(x_1, 0, 0) - \frac{1}{2}(2p + q + 1)\zeta^2 + \\ & + \frac{1}{2}(p - q - 1)y^2 + \frac{1}{2}pz^2 + s\zeta^3 - \\ & - \frac{3}{2}s\zeta y^2 - \frac{3}{2}s\zeta z^2 + \dots, \end{aligned} \quad (2.71)$$

correctly to terms of third order in x, y, z , where—as before— $\zeta \equiv x - x_1$ and where we have abbreviated

$$s = x_1^{-4} - q(1 - x_1)^{-4}. \quad (2.72)$$

Over an equipotential surface $\Psi = \text{constant}$ and, therefore, $\Psi(x, y, z) = \Psi(x_1, 0, 0)$. If, moreover, we confine our attention to an intersection of these equipotentials with the plane $z = 0$, Equation (2.72) can be solved for y in terms of ξ in the form

$$\begin{aligned} y^2 = & \frac{(2p + q + 1)\zeta^2 - 2s\zeta^3}{p - q - 1 - 3s\zeta} = \\ = & \frac{2p + q + 1}{p - q - 1} \zeta^2 + \frac{4p + 5q + 5}{(p - q - 1)^2} s\zeta^3 + \dots \end{aligned} \quad (2.73)$$

If we truncate the expansion on the r.h.s. of the foregoing equation to its first term, we obtain the osculating cone identical with Equation (2.62) above. The next term, factored by an odd power of ζ , will change sign as $x \gtrless x_1$: for $x < x_1$ (i.e., in the direction of the less massive star) it will be negative and, hence, the actual value of y^2 will be less than that appropriate for the osculating cone. For $x > x_1$ the converse will, however, be the case; and the actual Roche surface will overflow the osculating cone.

The extent to which this is the case cannot, in general, be established analytically, and recourse must be had to numerical computation. This has recently

q	ψ_{\max}	ψ_{cone}	i_{\min}	i_{cone}
1.00	57.31	57.31	34.45	34.45
0.80	57.35	57.32	34.45	34.45
0.60	57.49	57.35	34.33	34.44
0.40	57.88	57.43	34.07	34.42
0.20	59.00	57.64	33.34	34.35
0.10	60.56	57.92	32.39	34.27

Table II.4: Eclipse and osculating cone angles (in degrees) as a function of mass-ratio for binary systems in which both components fill their Roche lobes (after Chanan *et al*, 1976).

been done by Chanan *et al* (1976), from whose paper the data given in columns (2) and (4) of the accompanying Table II.4 have been excerpted. In the *conical* approximation, *the maximum duration of eclipse* (i.e., the maximum value of the phase angle ψ_1 of first contact of the eclipse) can be expressed in a closed form in the following manner. Let xy stand for the orbital plane of the two components, inclined to our normal to the line of sight (i.e., tangent to the celestial sphere) at an angle i . If so, then obviously

$$\left. \begin{aligned} x &= \cos \psi_1 \sin i \equiv \cos \epsilon, \\ y &= \sin \psi_1 \sin i, \\ z &= \cos i; \end{aligned} \right\} \quad (2.74)$$

and the apparent projected distance δ_1 between the centres of the two components at the phase angle ψ_1 will be given by

$$\delta_1^2 \equiv y^2 + z^2 = \sin^2 \psi_1 \sin^2 i + \cos^2 i. \quad (2.75)$$

Since, moreover,

$$1 - \delta_1^2 = \cos^2 \epsilon = \frac{1}{1 + \tan^2 \epsilon}, \quad (2.76)$$

a combination of (2.67) with (2.76) discloses that

$$\delta_1^2 = \frac{a \cos^2 i}{a - 1} \left\{ \frac{a + 2 - 4\delta_1^2}{a + 2 - 3\delta_1^2} \right\}, \quad (2.77)$$

where we have abbreviated

$$a \equiv \frac{q + 1}{p} = \frac{q + 1}{x_1^{-3} + q(1 - x_1)^{-3}} \quad (2.78)$$

by (2.64).

The maximum duration of the eclipse will occur when $i = 90^\circ$ and $Z \equiv \cos i = 0$. If so, however, Equation (2.77) can remain finite only if the denominator $a + 2 - 3\delta_1^2$ on the right-hand side of (2.77) will also vanish—which will be the case if

$$\delta_{\text{cone}}^2 \equiv \sin^2 \psi_{\text{cone}} = \frac{a + 2}{3} \quad (2.79)$$

yielding

$$\cos^2 \psi_{\text{cone}} = \frac{1 - a}{3} = \frac{p - q - 1}{3p}. \quad (2.80)$$

Conversely, the eclipse becomes grazing (i.e., $\delta_0 \equiv \cos i_{\text{min}}$) if $\psi = 0^\circ$. If so, however, Equation (2.77) will disclose that

$$\cos^2 i_{\text{cone}} = \frac{a + 2}{a + 3} = \frac{2p + q + 1}{3p + q + 1}. \quad (2.81)$$

The values of ψ and i_{cone} are then listed as functions of q in columns (3) and (5) of Table II.4. This is always bound to be true if the contact component of the Roche loop is the less massive one of the two; for the more massive component (i.e., the larger of the two, the values given in column (2) continue to apply.

A glance at these data discloses that *the values of ψ_{max} are remarkably insensitive to the mass-ratio*—a fact of considerable significance for the students of close binary systems, first noted by the present writer in 1954; for the variation of light exhibited by systems the components of which fill in the largest Roche lobes capable of containing their mass (in particular, eclipsing systems of the W UMa-type) in the course of an orbital cycle is so smooth and continuous that it is next to impossible to detect by a mere inspection of their respective light curves just where eclipses may set in. Our present analysis has now supplied a theoretical answer: namely, *the light changes of an eclipsing system will be unaffected by eclipses for all phase angles in excess of $\pm 60^\circ$ even if both components are in actual contact*—at least as long as their mass-ratios do not become less than 1:10 (though for greater disparity in masses this limit will continue to increase; cf. Chanan *et al.*, 1976). Therefore, the light changes exhibited at phases $\pm 30^\circ$ (or more) around each quadrature should be due solely to the proximity effects associated with both stars (cf. Chapter VII), and may be analysed as such without fear of interference from eclipse phenomena. Moreover—and again almost regardless of the mass ratio q —Equation (2.81) makes it evident that *no binary system can exhibit eclipses if its orbit is inclined to the celestial sphere by less than 33° – 34°* . For values of i greater than this limit eclipses may occur (and must occur for contact binary systems), of durations ψ_1 connected with i by Equation (2.77) in the conical approximation. For mass ratios $q \approx 1$ the relation between the two becomes again more involved; and for its tabulation the reader is referred to Chanan *et al.* (1976).

D: External Envelopes

In the foregoing parts of this section we have been concerned with various properties of Roche equipotentials when $\xi > \xi_1$, and later we investigated the geometry of limiting double-star configurations for which $\xi = \xi_1$. The aim of the present section will be to complete our analysis of the geometrical properties of the Roche model by considering what happens when $\xi < \xi_1$. In the introductory part of this chapter we inferred on general grounds that, if $\xi < \xi_1$, the dumb-bell figure which originally surrounded the two components will open up at P_1 (cf. again Figure II.1 and the corresponding equipotentials will enclose *both* bodies.

When will these latter equipotentials containing the total mass of our binary system cease to form a *closed* surface? A quest for the answer will take us back to Equation (2.20) defining the partial derivative ξ_x . We may note that the right-hand side of this equation is positive when $x \rightarrow \infty$, but becomes negative when $x = 1 + \epsilon$, where ϵ denotes a small positive quantity. It becomes positive again as $x \rightarrow 0$, and changes sign once more for $x \rightarrow -\infty$. Since ξ_x is finite and continuous everywhere except at $x = \infty$ and for $r = 0$ or $r' = 0$, it follows that it changes sign *three* times by passing through zero at points x_1, x_2, x_3 , whose values are such that

$$(a) \ 0 < x_1 < 1, \quad (b) \ x_2 > 1, \quad (c) \ x_3 < 0; \quad (2.82)$$

and of these, only the first one has been evaluated so far in this section, and its numerical values listed in column (2) of Table II.1.

An evaluation of the remaining roots $X_{2,3}$ offers, however, no greater difficulty. In embarking upon it we should merely keep in mind that, regardless of the sign of x , the distances r and r' as defined by Equations (1.3) are *positive* quantities. Thus, unlike in case (a)—when, by setting $r = x$ and $r' = 1 - x$, we were led to define x_1 as a root of Equation (2.24)—in case (b), when $x_2 > 1$, we must set $r = x$ but $r' = x - 1$; and in case (c), when $x_3 < 0$, $r = -x$ and $r' = 1 - x$. After doing so and clearing the fractions we may verify that the equation $\xi_x = 0$ in the case of (b) and (c) assumes the explicit form

$$(1 + q)x^5 - (2 + 3q)x^4 + (1 + 3q)x^3 - (1 + 2q)x^2 + 2x - 1 = 0 \quad (2.83)$$

and

$$(1 + q)x^5 - (2 + 3q)x^4 + (1 + 3q)x^3 + x^2 - 2x + 1 = 0, \quad (2.84)$$

respectively

For $q = 0$, the former Equation (2.83) becomes identical with (2.24) and reduces to (2.25) admitting of $x = 1$ as a triple root. Hence, for small values of q , the root $x_2 > 1$ of the complete Equation (2.83) should be expandible as

$$x_2 = 1 + \left(\frac{\mu}{3}\right)^{1/3} + \frac{1}{3}\left(\frac{\mu}{3}\right)^{2/3} + \frac{1}{9}\left(\frac{\mu}{3}\right) + \dots \quad (2.85)$$

in terms of fractional powers of $\mu \equiv q/(q+1)$. Similarly, Equation (2.84) reduces for $q = 0$ to

$$(x - 1)^2(x^3 + 1) = 0, \quad (2.86)$$

admitting of only one negative root (namely, -1). In consequence, the negative root x_3 of (2.84) should, for small values of μ , be approximable in terms of integral powers of μ by an expansion of the form

$$x_3 = -1 + \frac{7}{12}\mu - \frac{1127}{20736}\mu^3 + \dots \quad (2.87)$$

The approximate values of x_2 and x_3 as obtained from (2.85)–(2.87) may, moreover, be subsequently refined to any degree of accuracy by differential corrections or any other standard method.

Once sufficiently accurate values of $x_{2,3}$ have thus been established, the values of ξ corresponding to equipotentials which pass through these points can be ascertained from the equation

$$\xi_{2,3} = \xi(x_{2,3}, 0, 0); \quad (2.88)$$

while the corresponding values of $C_{2,3}$ then can be found (cf. Equation (2.31) from

$$C_{2,3} = 2(1 - \mu)\xi_{2,3} + \mu_2. \quad (2.89)$$

A tabulation of five-digit values of $x_{2,3}$ and $C_{2,3}$ is given in columns (2)–(5) of the accompanying Table II.5. It may also be noticed that, to a high degree of approximation

$$\xi_3 \doteq \frac{3}{2} + 2q - \frac{q^2}{2(1+q)} \quad (2.90)$$

or

$$C_3 \doteq 3 + \mu; \quad (2.91)$$

while, somewhat less accurately,

$$(x_2 - 1)^2 = 1 - x_3^2. \quad (2.92)$$

A comparison of the values of $C_{2,3}$ as given in Table II.5 with those of C_1 from Table II.2 reveals that, for all values of $q > 0$,

$$C_1 > C_2 \geq C_3. \quad (2.93)$$

For any value of C within the limits of the inequality $C_1 > C > C_2$ the corresponding equipotential will surround the whole mass of the system by a common *external envelope*, which may enclose the common atmosphere of the two stars. For $C = C_2$, this envelope will develop a conical point P_2 (at which $\xi_x = \xi_y = \xi_z = 0$) at $x = x_2$ —i.e., behind the centre of gravity of the less massive component (see Figures II.1 or II.2); and if $C < C_2$, the respective equipotentials will open up at P_2 . For $C = C_3$, a third conical point P_3 develops behind the centre of gravity of the more massive component at $x = x_3$; and if $C < C_3$, the equipotentials will open up at both ends. Their intersection with the xy -plane will then no longer represent a single closed curve, but will split up in two separate sections (symmetrical with respect to the x -axis), closing gradually around

q	x_2	C_2	$-x_3$	C_3	$C_{4,5}$
1.0	1.69841	3.45680	0.69841	3.45680	2.75000
0.8	1.66148	3.49368	0.73412	3.41509	2.75309
0.6	1.61304	3.53108	0.77751	3.35791	2.76563
0.4	1.54538	3.55894	0.83180	3.27822	2.79592
0.3	1.49917	3.55965	0.86461	3.22675	2.82249
0.2	1.43808	3.53634	0.90250	3.16506	2.86111
0.15	1.39813	3.50618	0.92372	3.12959	2.88658
0.1	1.34700	3.45153	0.94693	3.09058	2.91735
0.05	1.27320	3.34671	0.97222	3.04755	2.95465
0.02	1.19869	3.22339	0.98854	3.01961	2.98077
0.01	1.15614	3.15344	0.99422	3.00990	2.99020
0.005	1.12294	3.10301	0.99710	3.00498	2.99504
0.001	1.07089	3.03838	0.99942	3.00099	2.99990
0.0002	1.04108	3.01387	0.99988	3.00020	2.99980
0	1.00000	3.00000	1.00000	3.00000	3.00000

Table II.5: The data collected in this table are taken from Kopal (1959). For other tabulations of these quantities—in particular for very small values of the parameter $\mu = q/(q + 1)$ —cf., Rosenthal (1931), Kuiper and Johnson (1956), Szebehely (1967) or Kitamura (1970).

two points which make equilateral triangles with the centres of mass of the two components. The coordinates of such points are specified by the requirements that $r = r' = 1$; consequently, $x = 0.5$ and $y = \pm\sqrt{3}/2$. These triangular points represent also the loci at which our equipotentials vanish eventually from the real plane — if (consistent with Equations 1.6 and 2.31) their constants C reduce to

$$C_{4,5} = 3 - \mu + \mu^2. \quad (2.94)$$

The values of $C_{4,5}$'s as given by this equation are listed in column (6) of Table II.5 for $1 > q > 0$, and represent the lower limits attainable by these constants; for if $C < C_{4,5}$, the equipotential curves $\xi = \text{constant}$ in the xy -plane become imaginary, and thus devoid of any physical significance.

II.3 Time-Dependent Roche Equipotentials

The geometrical properties of equipotential surfaces surrounding the Roche gravitational dipoles discussed in the preceding section, are independent of the time. This is, however, true only within the framework of special assumptions underlying Equation (1.6): namely, for constant values of $m_{1,2}$ and R (i.e., if the two finite masses describe circular orbits with the Keplerian angular velocity $\omega \equiv \omega_K$), and if the equatorial plane of the rotating configuration coincides with that of their orbit. A breakdown of any of these assumptions is, however, bound to render the expression for the total potential Ψ as given by Equation (1.2)—and, consequently, the normalized potential ξ —a function of time; and the aim of the present section will be to develop the necessary consequences of this fact.

A: Inclined Axes of Rotation

In order to investigate such effects, consider first the case in which the component of mass m_1 (whose equipotential surfaces are distorted by tides raised by its companion of mass m_2) rotates about an arbitrarily oriented axis with an angular velocity ω_1 which may (but need not) be equal to the Keplerian angular velocity ω_K as given by Equation (1.4). If so, Equation (1.2) for the total potential Ψ should be replaced by

$$\begin{aligned} \Psi = & G \frac{m_1}{r} + G \frac{m_2}{r'} + \frac{\omega_K^2}{2} \left(\frac{m_2 R}{m_1 + m_2} \right)^2 - \\ & - \omega_K^2 \left(\frac{m_2 R}{m_1 + m_2} \right) x'' + \frac{\omega_1^2}{2} (x'^2 + y'^2), \end{aligned} \quad (3.1)$$

where the singly-primed rectangular coordinates x', y', z' rotate with the angular velocity ω_1 of the star of mass m_1 , but x'' stands for the *revolving* coordinate the axis of which coincides with the radius-vector r of relative orbit of the two finite masses m_1 and m_2 .

In order to relate the singly- and doubly-primed coordinates with each other, consider (also for future use) three systems of rectangular coordinates, defined as follows:

1) The (unprimed) axes XYZ will represent a system of *inertial* coordinates (“space axes”) of direction fixed in space in such a way that the XY -plane coincides with the *invariable plane of the system*; while the Z -axis is perpendicular to it.

2) The singly-primed axes $X'Y'Z'$ will stand for a system of rectangular coordinates *rotating* with the body (“body-axes”), defined so that $X'Y'$ -plane represents the (instantaneous) *equator* of the rotating star, inclined by an angle θ to the inertial XY -plane and intersecting it at the angle ϕ (see Figure II.3).

3) The doubly-primed axes $X''Y''Z''$ will hereafter represent a system of *revolving* rectangular coordinates, in which the X -axis is constantly coincident with the radius-vector between the origin and the centre of mass of the revolving star,

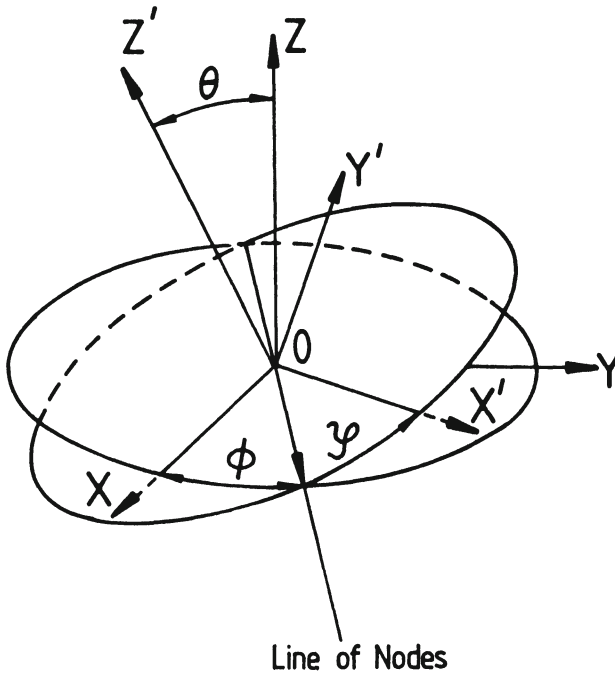


Figure II.3: Definition of Eulerian angles

and $Z'' = 0$ represents the (instantaneous) position of its orbital plane. As is well known, a transformation of coordinates from the inertial (space) to the rotating (body) axes is governed by the matrix equation

$$\begin{Bmatrix} x \\ y \\ z \end{Bmatrix} = \begin{Bmatrix} a'_{11} & a'_{12} & a'_{13} \\ a'_{21} & a'_{22} & a'_{23} \\ a'_{31} & a'_{32} & a'_{33} \end{Bmatrix} \begin{Bmatrix} x' \\ y' \\ z' \end{Bmatrix}, \quad (3.2)$$

where the direction cosines

$$\left. \begin{aligned} a'_{11} &= \cos \varphi \cos \phi - \sin \varphi \sin \phi \cos \theta, \\ a'_{12} &= -\sin \varphi \cos \phi - \cos \varphi \sin \phi \cos \theta, \\ a'_{13} &= \sin \phi \sin \theta; \end{aligned} \right\} \quad (3.3)$$

$$\left. \begin{aligned} a'_{21} &= \cos \varphi \sin \phi + \sin \varphi \cos \phi \cos \theta, \\ a'_{22} &= -\sin \varphi \sin \phi + \cos \varphi \cos \phi \cos \theta, \\ a'_{23} &= -\cos \phi \sin \theta; \end{aligned} \right\} \quad (3.4)$$

$$\left. \begin{aligned} a'_{31} &= \sin \varphi \sin \theta, \\ a'_{32} &= \cos \varphi \sin \theta, \\ a'_{33} &= \cos \theta; \end{aligned} \right\} \quad (3.5)$$

where the Eulerian angles ϕ, θ, φ are defined by a scheme illustrated on Figure II.3.

A transformation of the inertial to revolving coordinates is similarly governed by the matrix equation

$$\begin{Bmatrix} x \\ y \\ z \end{Bmatrix} = \begin{Bmatrix} a''_{11} & a''_{12} & a''_{13} \\ a''_{21} & a''_{22} & a''_{23} \\ a''_{31} & a''_{32} & a''_{33} \end{Bmatrix} \begin{Bmatrix} x'' \\ y'' \\ z'' \end{Bmatrix}, \quad (3.6)$$

where the direction cosines

$$\begin{Bmatrix} a''_{11} = \cos u \cos \Omega - \sin u \sin \Omega \cos i, \\ a''_{12} = -\sin u \cos \Omega - \cos u \sin \Omega \cos i, \\ a''_{13} = \sin \Omega \sin i; \end{Bmatrix} \quad (3.7)$$

$$\begin{Bmatrix} a''_{21} = \cos u \sin \Omega + \sin u \cos \Omega \cos i, \\ a''_{22} = -\sin u \sin \Omega + \cos u \cos \Omega \cos i, \\ a''_{23} = -\cos \Omega \sin i; \end{Bmatrix} \quad (3.8)$$

$$\begin{Bmatrix} a''_{31} = \sin u \sin i, \\ a''_{32} = \cos u \sin i, \\ a''_{33} = \cos i; \end{Bmatrix} \quad (3.9)$$

where Ω denotes the longitude of the nodes (i.e., of intersection of the $Z = 0$ and $Z'' = 0$ planes measured from the X -axis); i , the inclination of the orbital ($Z'' = 0$) to the invariable ($Z = 0$) plane of the system; and u , the angle between the line of the nodes and the instantaneous position of the radius-vector (if, in Equations (3.3)–(3.5) defining the singly-primed direction cosines a'_{ij} , we set $\phi = \Omega, \varphi = u$ and $\theta = i$, the a'_{ij} 's become identical with the doubly-primed direction cosines a''_{ij}).

Accordingly, a transformation from the rotating (singly-primed) to the revolving (doubly-primed) axes obeys the matrix equation

$$\begin{Bmatrix} x' \\ y' \\ z' \end{Bmatrix} = \begin{Bmatrix} \lambda''_1 & \lambda''_2 & \lambda''_3 \\ \mu''_1 & \mu''_2 & \mu''_3 \\ \nu''_1 & \nu''_2 & \nu''_3 \end{Bmatrix} \begin{Bmatrix} x'' \\ y'' \\ z'' \end{Bmatrix} \quad (3.10)$$

where (cf. p.155 of Kopal, 1978)

$$\begin{Bmatrix} \lambda''_j \\ \mu''_j \\ \nu''_j \end{Bmatrix} = \begin{Bmatrix} a'_{11} & a'_{21} & a'_{31} \\ a'_{12} & a'_{22} & a'_{32} \\ a'_{13} & a'_{23} & a'_{33} \end{Bmatrix} \begin{Bmatrix} a''_{1j} \\ a''_{2j} \\ a''_{3j} \end{Bmatrix} \quad (3.11)$$

for $j = 1, 2, 3$ — so that the direction cosines $\nu''_{1,2,3}$ of the axis Z' in the doubly-primed revolving system

$$\begin{aligned} \nu''_1 &= a'_{13}a''_{11} + a'_{23}a''_{21} + a'_{33}a''_{31} \\ &\equiv \mathcal{A} \sin u + \mathcal{B} \cos u, \end{aligned} \quad (3.12)$$

$$\begin{aligned} \nu_2'' &= a'_{13}a''_{12} + a'_{23}a''_{22} + a'_{33}a''_{32} \\ &\equiv \mathcal{A} \cos u - \mathcal{B} \sin u, \end{aligned} \quad (3.13)$$

$$\begin{aligned} \nu_3'' &= a'_{13}a''_{13} + a'_{23}a''_{23} + a'_{33}a''_{33} \\ &\equiv (1 - \mathcal{A}^2 - \mathcal{B}^2)^{1/2}, \end{aligned} \quad (3.14)$$

where we have abbreviated

$$\mathcal{A} = \cos \theta \sin i - \sin \theta \cos(\phi - \Omega) \cos i, \quad (3.15)$$

$$\mathcal{B} = \sin \theta \sin(\phi - \Omega); \quad (3.16)$$

such that

$$(1 - \mathcal{A}^2 - \mathcal{B}^2)^{1/2} = \cos \theta \sin i + \sin \theta \cos(\phi - \Omega) \sin i \equiv \nu_3''. \quad (3.17)$$

The foregoing Equations (3.16)–(3.17) for $\nu_{1,2,3}''$ are exact for any values of the Eulerian angle θ or the inclination i . If, however, we identify the Z'' -axis with Z —i.e., set $i = 0$ rendering $Z'' = 0$ the invariable plane of the respective system (an identification permissible without any loss of generality for the Roche model, though *not* for one exhibiting a finite degree of central condensation; cf. Section VI.3A), Equations (3.12) – (3.14) will reduce to

$$\left. \begin{aligned} \nu_1'' &= -\sin \theta \sin(u + \Omega - \phi), \\ \nu_2'' &= -\sin \theta \cos(u + \Omega - \phi), \\ \nu_3'' &= +\cos \theta; \end{aligned} \right\} \quad (3.18)$$

in which the Eulerian angles θ and ϕ of Figure II.3 as well as the longitude Ω of the nodes at which the planes $Z = Z'' = 0$ intersect can be treated as constants.

After these preliminaries let us return to Equation (3.1) for the generalized potential with inclined axes of rotation, and rewrite the expression $x'^2 + y'^2$ on the r.h.s. of (3.1) in terms of the revolving coordinates x'', y'', z'' by means of the transformation (3.10): in doing so we find that

$$\begin{aligned} x'^2 + y'^2 &= r^2 - (\nu_1''x'')^2 - (\nu_2''y'')^2 - (\nu_3''z'')^2 - \\ &\quad - 2(\nu_1''\nu_2''x''y'' + \nu_1''\nu_3''x''z'' + \nu_2''\nu_3''y''z''), \end{aligned} \quad (3.19)$$

$r^2 = x''^2 + y''^2 + z''^2$ exactly; or, alternatively,

$$x'^2 + y'^2 = r^2(1 - \cos^2 \Theta) = \frac{2}{3} [1 - P_2(\cos \Theta)] \quad (3.20)$$

where

$$\cos \Theta = \lambda''\nu_1'' + \mu''\nu_2'' + \nu''\nu_3''; \quad (3.21)$$

and λ'', μ'', ν'' being the direction cosines of an arbitrary radius-vector r in the doubly-primed coordinates. Accordingly (by the addition theorem for the Legendre coefficients)

$$\begin{aligned} P_2(\cos \Theta) &= P_2(\cos \theta)P_2(\cos \theta'') + \\ &+ \frac{1}{3}P_2^1(\cos \theta)P_2^1(\cos \theta'') \sin(\phi - \Omega - u - \phi'') - \\ &- \frac{1}{12}P_2^2(\cos \theta)P_2^2(\cos \theta'') \cos 2(\phi - \Omega - u - \phi''); \end{aligned} \quad (3.22)$$

and if, moreover, the Eulerian angle θ is small enough for its squares and higher powers to be ignorable, the foregoing expression simplifies to

$$P_2(\cos \Theta) = P_2(\nu'') + 3\lambda''\mu'' \sin \theta \sin(\phi - \Omega - u) - 3\mu''\nu'' \sin \theta \cos(\phi - \Omega - u) + \dots \quad (3.23)$$

When $\theta = 0$ (i.e., if the equator and orbit are coplanar), $\cos \Theta$ becomes identical with ν'' as it was in Section II.1; but for $\theta \neq 0$, $\cos \Theta$ turns out to depend on the true anomaly u measured from the node. If, moreover, $\omega_1 = \omega_K$, we can set $\phi = \Omega$; but otherwise this need not be the case (cf. Chapter VI).

However, the presence of extra terms on the right-hand side of the Equation (3.1) for the Roche equipotentials—rendering the latter to depend on the time—will also influence the explicit form of the expansion (2.12) of their radius-vector r in ascending powers of r_0 : in fact, proceeding in the same way as in Section II.2A we find that (correctly to terms of the order of r_0^5) the right-hand side of Equation (2.12) should be augmented by the term

$$+ nr_0^3(\omega_1/\omega_K)^2(1 - \cos^2 \Theta), \quad (3.24)$$

where (by Equation (3.21)),

$$\cos \Theta = \cos \theta \cos \theta'' + \sin \theta \sin \theta'' \sin(\phi - \Omega - u - \phi'') \quad (3.25)$$

replacing $nr_0^2(1 - \cos^2 \theta'')$; but an evaluation of higher-order effects arising from inclination of the equator to the orbital plane should be left as an exercise for the interested reader.

B: Eccentric Orbits

In conclusion of our brief survey of different geometrical properties of the Roche Model, let us point out one additional case in which such properties are bound to depend on the time: namely, if the Keplerian orbit of the two finite masses m_1 and m_2 becomes eccentric. If so, the separation R of their mass centres will be bound to vary as

$$R = \frac{A(1 - e^2)}{1 + e \cos v}, \quad (3.26)$$

where A stands for the semi-major axis of relative orbit of the masses $M_{1,2}$; e , its eccentricity; and v is the true anomaly measured from the periastron passage. Within the framework of the Roche model (i.e., if $m_{1,2}$ can be regarded as mass-points) the parameters A and e on the right-hand side can be regarded as constants. If so, the right-hand side of the expression (1.2) for the total potential Ψ can be rewritten, more explicitly, as

$$\frac{\Psi(v)}{G(m_1 + m_2)} = \frac{1 - \mu}{r} + \frac{\mu}{R} \left\{ 1 + \left[1 - \left(\frac{R}{A} \right)^3 \right] \frac{x}{r} + \sum_{j=2}^{\infty} \left(\frac{r}{R} \right)^j P_j \left(\frac{x}{r} \right) \right\} + \frac{x^2 + y^2}{2A^3} + \frac{\mu^2 R^2}{2A^3}, \quad (3.27)$$

where (in agreement with Equations (2.32)) $\mu \equiv m_2/(m_1 + m_2)$; and for eccentric orbits, the Keplerian angular velocity

$$\omega_K^2 = \frac{G(m_1 + m_2)}{A^3}. \quad (3.28)$$

We wish to conclude this chapter by a proof that, in the case of elliptic orbits of masses $m_{1,2}$, the foregoing potential (3.27) is no longer identical with the zero-velocity surfaces of the restricted problem of three bodies. In order to do so, let us depart from the elliptic three-body problem in space, which in the revolving (doubly-primed) coordinates x'', y'', z'' assumes the form

$$\ddot{x}'' - 2\dot{y}'' = (1 + e \cos v)^{-1} \Omega_{x''}, \quad (3.29)$$

$$\ddot{y}'' + 2\dot{x}'' = (1 + e \cos v)^{-1} \Omega_{y''}, \quad (3.30)$$

$$\ddot{z}'' = (1 + e \cos v)^{-1} \Omega_{z''}; \quad (3.31)$$

in terms of the potential

$$\Omega = (1 - \mu)(r_1^{-1} + \frac{1}{2}r_1^2) + \mu(r_2^{-1} + \frac{1}{2}r_2^2) - \frac{1}{2}z''^2(1 + e \cos v); \quad (3.32)$$

or, alternatively,

$$\ddot{x}'' - 2\dot{y}'' = (1 + e \cos v)^{-1} \Omega'_{x''}, \quad (3.33)$$

$$\ddot{y}'' + 2\dot{x}'' = (1 + e \cos v)^{-1} \Omega'_{y''}, \quad (3.34)$$

$$\ddot{z}'' + z'' = (1 + e \cos v)^{-1} \Omega'_{z''}, \quad (3.35)$$

where

$$\begin{aligned} \Omega' &= \Omega + \frac{1}{2}z''^2(1 + e \cos v) = \\ &= (1 - \mu)(r_1^{-1} + \frac{1}{2}r_1^2) + \mu(r_2^{-1} + \frac{1}{2}r_2^2), \end{aligned} \quad (3.36)$$

in which

$$r_1^2 = (x'' + \mu)^2 + y''^2 + z''^2 \quad (3.37)$$

and

$$r_2^2 = (x'' + \mu - 1)^2 + y''^2 + z''^2 ; \quad (3.38)$$

differing from r and r' as defined by Equations (1.3) only insofar as the origin of coordinates has been shifted from the centre of mass m_1 to that of the system $m_1 m_2$ as a whole.

The dots on the left-hand sides of Equations (3.31)–(3.32) or (3.35)–(3.36) stand for ordinary differentiation with respect to the time t , and the terms factored by \dot{x} and \dot{y} represent the effects of the Coriolis force. It may also be noted that the potential Ω' as defined by Equation (3.36) does not depend explicitly on the eccentricity e of the orbit of the finite masses m_1 and m_2 ; nor does it depend explicitly on the time; the latter enters Equations (3.35)–(3.37) only through the cosine of the true anomaly v of the binary orbit.

In order to obtain the Jacobi energy integral of the systems (3.31)–(3.32) or (3.35)–(3.36), let us multiply these equations successively by \dot{x} , \dot{y} , \dot{z} and add: the result will be (in each case)

$$\begin{aligned} \frac{1}{2} \frac{d}{dt} (\dot{x}''^2 + \dot{y}''^2 + \dot{z}''^2 + z'') &= (1 + e \cos v)^{-1} (\dot{x}'' \Omega_{x''} + \dot{y}'' \Omega_{y''} + \dot{z}'' \Omega_{z''}) \\ &= (1 + e \cos v)^{-1} \frac{d\Omega}{dt} \end{aligned} \quad (3.39)$$

or

$$\frac{1}{2} \frac{d}{dt} \{(\dot{x}'')^2 + (\dot{y}'')^2 + (\dot{z}'')^2\} = (1 + e \cos v)^{-1} \frac{d\Omega'}{dt} . \quad (3.40)$$

If, moreover, we change over from the time t to the true anomaly v as the independent variable of our problem by means of Kepler's second law

$$r^2 dv = \sqrt{G(m_1 + m_2)} dt \quad (3.41)$$

valid for the orbit of the two finite masses, Equation (3.39) can be formally integrated to yield

$$(\dot{x}'')^2 + (\dot{y}'')^2 + (\dot{z}'')^2 + (z'')^2 = 2 \int \frac{d\Omega}{1 + e \cos v} \quad (3.42)$$

or

$$(\dot{x}'')^2 + (\dot{y}'')^2 + (\dot{z}'')^2 = 2 \int \frac{d\Omega'}{1 + e \cos v} . \quad (3.43)$$

For $e = 0$ (corresponding to a "circular" restricted problem of three bodies), the foregoing Equations (3.42) and (3.43) can be readily integrated to yield

$$T = \Omega + C , \quad (3.44)$$

where

$$T = \frac{1}{2} \{(\dot{x}'')^2 + (\dot{y}'')^2 + (\dot{z}'')^2\} \quad (3.45)$$

stands for the (scaled) kinetic energy of the system; Ω , for its potential energy; and C is a constant of integration independent of the time.

Equation (3.44) as it stands represents the classical form of the Jacobi integral of the “circular” restricted problem of three bodies. If, however, $e \neq 0$, it is no longer admissible to integrate Equations (3.39) or (3.40) explicitly to the form (3.42) or (3.43): the latter become mere identities, satisfied by any solution of the Equations (3.31)–(3.32) or (3.35)–(3.36) of motion. The significance of the classical Jacobi integrals rests on the fact that, if $e = 0$, each side of Equations (3.42) or (3.43) constitutes a perfect differential; so that the values of the various terms depend only on the end-point positions of the infinitesimal mass particle. But if $e > 0$, in order to establish the instantaneous shape of the zero-velocity surface, we would need to know the value of $d\Omega$ at each value of (or v) all along any selected path; and to establish this from (3.42) or (3.43), an integration of Equations (3.31)–(3.33) or (3.35)–(3.37) would require the adoption of six arbitrary constants representing the initial conditions of our problem; and no closed formula can be invoked to establish the outcome.

Only in our particular case do the known solutions of the “circular” problem of three bodies transfer readily to the “elliptical” case: namely, the positions of the five Lagrangian points in the orbital plane of the two finite masses. As is well known, their locations are defined by the requirements that the velocities as well as accelerations vanish simultaneously at such points in the plane $z'' = 0$; and if so, the left-hand sides of Equations (3.31)–(3.33) or (3.35)–(3.37) vanish identically. However, in order that this be true, it is necessary that their right-hand sides must vanish—i.e., that

$$\Omega'_{x''} = \Omega'_{y''} = \Omega'_{z''} = 0 \quad (3.46)$$

as well; and the coordinates x'' , y'' at which this occurs for $z'' = 0$ have already been established in Section 2C of this chapter. We stressed, however, before that the potential Ω' of the “elliptic” problem as given by Equation (3.36) is independent of the eccentricity of the Keplerian orbit of the finite masses m_1 and m_2 —a fact which implies that the existence as well as relative positions of the five Lagrangian points—collinear as well as triangular—remains the same as given in Table II.5; and completely independent of e .

II.4 Bibliographical Notes

The contents of Sections 1 and 2 of this chapter follow largely the presentation of the subject in the first part of Chapter VI of the writer’s *Dynamics of Close Binary Systems* (Kopal, 1978) and (partly) Chapter III of his previous treatise (Kopal, 1959); with corrections of misprints which crept into these previous sources. The geometry of the eclipses of contact systems represented by the Roche model can be traced to a previous source (Kopal, 1954); while for complications arising from a great disparity in mass-ratios of contact systems see Chanan, Middleditch and Nelson (1976).

It may be noted that the term “Roche Limit” in the sense used in this book (as well as in all other above-quoted sources) goes back to Kopal (1955). It is not to be mistaken

for the concept signifying the minimum distance at which a fluid satellite of infinitesimal mass can approach an oblate planet (Roche, 1850), and referred to as "Roche Limit" by G. H. Darwin (1906, 1911) and Jeans (1919). In this sense, it likewise continues to be used (cf. Chandrasekhar, 1963; or Kopal and Song, 1983) up to the present time.

For previous literature concerning the time-dependent Roche equipotentials discussed in Section II.3A, cf. Plavec (1958); Limber (1963) or Kruszewski (1966).

Concerning the "elliptic" restricted problem of three bodies, the equations (3.35)–(3.37) used in Section II.3B were deduced first by Scheibner as far back as 1866. However, inasmuch as Scheibner's work appeared in a non-astronomical periodical and under a concealing title ("Satz aus der Störungstheorie"), it was generally overlooked by subsequent investigators, and remained unknown until it was re-discovered independently by Nechvíle (1926) and Rein (1940).

For the energy integral of the elliptic problem of three bodies cf. Ovenden and Roy (1961) or Kopal and Lyttleton (1963). A treatment of this subject in Section II.3B follows largely this latter source.